J|A|C|S
ARTICLES
Published on Web 08/15/2007

Ultrafast Energy Transfer and Strong Dynamic Non-Condon Effect on Ligand Field Transitions by Coherent Phonon in γ-Fe_2O_3 Nanocrystals

Tai-Yen Chen, Chih-Hao Hsia, Hyung Su Son, and Dong Hee Son*

Contribution from the Department of Chemistry, Texas A&M University, College Station, Texas 77842

Received April 12, 2007; E-mail: dhson@mail.chem.tamu.edu

Abstract: Relaxation dynamics of an optically excited ligand field state and strong modulation of oscillator strengths of ligand field transitions by coherent acoustic phonon in γ-Fe_2O_3 nanocrystals were investigated through transient absorption measurements. A near-infrared pump beam prepared the lowest excited ligand field state of Fe^{3+} ions preferentially on the tetrahedral coordination site. A time-delayed visible probe beam monitored the dynamics of various ligand field transitions and modification of their oscillator strengths by a coherent lattice motion. Transient absorption data exhibited dynamic features of a few distinct time scales, 100 fs, 1 ps, and 17−100 ps, as well as intense oscillatory features resulting from a coherent acoustic phonon. The initial decay of the induced absorption in 100 fs has been attributed to the exchange interaction-mediated energy transfer from the tetrahedral to octahedral Fe^{3+} sites. The dynamics of slower time scales were assigned to the vibrational and electronic relaxations. Excitation of the ligand field state created a coherent acoustic phonon resulting in unusually intense modulation of the transient absorption signal despite its predominantly local nature and relatively small vibronic coupling. Excitation of each Fe^{3+} ion in the nanocrystal was estimated to modulate up to 60% of its contribution to the total absorption intensity of the nanocrystal. The intense modulation of the absorption has been attributed to the strongly modulated oscillator strength of the ligand field transitions rather than oscillating Frank−Condon overlap. Dynamic modification of the metal−ligand orbital overlap and exchange interaction between the neighboring metal ions are the main factors responsible for the modulation of the oscillator strength.

1. Introduction

Transition metal oxides exhibit interesting magnetic, electronic, and optical properties that have been utilized in a variety of applications such as magnetic resonance imaging, catalysis, and solar cells.[1−4] Many of the electronic and magnetic properties of transition metal oxides are ruled by the electronic and spin states of d-electrons on the transition metal ions under the influence of the ligand field provided by oxygen ions.[5] The ligand field introduces a varying degree of periodic potential to d-electrons, thereby affecting their electronic and spin states. The state of d-electrons can be varied by many means such as direct optical excitation and modification of the ligand field via application of the pressure and temperature.[6−8] Optical excitation with ultrashort pulses, in particular, can directly access many ligand field states and modify electronic and magnetic properties in a very fast time scale. For instance, insulator−conductor phase transition and changes in magnetism in a subpicosecond time scale have been recently demonstrated in bulk transition metal oxides.[9,10]

It is important to note that an ultrashort optical excitation is often accompanied by coherent lattice motions, i.e., coherent phonons, through electron−phonon coupling in crystalline solids of various dimensionality.[11−13] While it may be less efficient than the charge-transfer transitions that are usually exploited to create coherent nuclear motions, ligand field transitions are also capable of exciting coherent phonons in principle. Excitation of coherent phonons can have a significant consequence on the properties of optically excited transition metal oxides because they can directly influence the ligand field strength acting on the transition metal ions. The influence of the coherent phonon on the material properties can be more pronounced in nanocrystals than in bulk because the energy barrier for various processes involving atomic motions in nanocrystals are typically

(1) Lee, J. H.; Huh, Y. M.; Jun, Y.; Seo, J.; Jang, J.; Song, H. T.; Kim, S.; Cho, E. J.; Yoon, H. G.; Suh, J. S.; Cheon, J. *Nat. Med.* **2007**, *13*, 95−99.
(2) Liu, H. Y.; Gao, L. *J. Am. Ceram. Soc.* **2006**, *89*, 370−373.
(3) Jiang, Y.; Decker, S.; Mohs, C.; Klabunde, K. J. *J. Catal.* **1998**, *180*, 24−35.
(4) Oregan, B.; Gratzel, M. *Nature* **1991**, *353*, 737−740.
(5) Tokura, Y.; Nagaosa, N. *Science* **2000**, *288*, 462−468.
(6) Gomez-Abal, R.; Ney, O.; Satitkovitchai, K.; Hubner, W. *Phys. Rev. Lett.* **2004**, *92*, 227402.
(7) Takano, M.; Nasu, S.; Abe, T.; Yamamoto, K.; Endo, S.; Takeda, Y.; Goodenough, J. B. *Phys. Rev. Lett.* **1991**, *67*, 3267−3270.
(8) Walz, F. *J. Phys.: Condens. Matter* **2002**, *14*, R285−R340.
(9) Kimel, A. V.; Kirilyuk, A.; Usachev, P. A.; Pisarev, R. V.; Balbashov, A. M.; Rasing, T. *Nature* **2005**, *435*, 655−657.
(10) Cavalleri, A.; Dekorsy, T.; Chong, H. H. W.; Kieffer, J. C.; Schoenlein, R. W. *Phys. Rev. B* **2004**, *70*, 161102R.
(11) Lindenberg, A. M.; Kang, I.; Johnson, S. L.; Missalla, T.; Heimann, P. A.; Chang, Z.; Larsson, J.; Bucksbaum, P. H.; Kapteyn, H. C.; Padmore, H. A.; Lee, R. W.; Wark, J. S.; Falcone, R. W. *Phys. Rev. Lett.* **2000**, *84*, 111−114.
(12) Bargheer, M.; Zhavoronkov, N.; Gritsai, Y.; Woo, J. C.; Kim, D. S.; Woerner, M.; Elsaesser, T. *Science* **2004**, *306*, 1771−1773.
(13) Krauss, T. D.; Wise, F. W. *Phys. Rev. Lett.* **1997**, *79*, 5102−5105.

10.1021/ja072578f CCC: $37.00

lower than in bulk.[14,15] In addition, the time scale of the lattice motion, particularly for an acoustic phonon, is dependent on the size of the nanocrystals, which provides an additional control in the dynamic modification of the material properties.[16−18] So far, the excitation of coherent acoustic phonon and its influence on the optical properties in nanocrystals were observed only in metal and semiconductor nanocrystals. Plasmonic or excitonic transition in metal and semiconductor nanocrystals created coherent acoustic phonons via impulsive heating or a displacive mechanism, inducing periodic shift of an exciton resonance peak or band gap. While a number of studies investigated the ultrafast electronic relaxation dynamics of the ligand field states in transition metal oxide nanocrystals, observation of the coherent phonons has not been reported so far.[19,20]

Here, we report the first observation of the coherent phonon and its influence on the optical properties in transition metal oxide nanocrystals created by the ultrafast excitation of the ligand field transition. Our interest in this study is investigating the influence of the coherent lattice motion on the optical properties of transition metal oxide nanocrystals, particularly on the properties of ligand field transitions. In this study, we focused our discussion on two main issues: (i) relaxation dynamics of the optically excited ligand field state, and (ii) effect of coherent phonons on ligand field transition strength. In this study, we chose γ-Fe_2O_3 as a model system of nanocrystalline transition metal oxides for which synthetic methods of making size-controlled and monodisperse nanocrystals are well established. An ultrafast near-infrared pump pulse prepared the lowest excited ligand field state ($^4T_1$) from the ground state ($^6A_1$). The transition energy is well separated from the charge-transfer transition above 4 eV, avoiding interference from the intense charge transfer absorption. Through time-resolved absorption measurements in the visible region, ultrafast (100 fs) energy transfer between Fe^{3+} ions on different coordination sites and the subsequent vibrational (1 ps) and electronic (100 ps) relaxation dynamics were observed. Furthermore, intense particle size dependent oscillations in the transient absorption data, due to the excitation of a coherent acoustic phonon, were observed in the entire visible region covering many ligand field transitions. Excitation of each Fe^{3+} ion in a nanocrystal was found to modulate up to 60% of its contribution to the overall absorption intensity of the nanocrystal. The large modulation of the absorption intensity has been attributed to the strongly modulated oscillator strength rather than oscillating Frank−Condon overlap. This study demonstrates that a direct optical excitation of a ligand field state can efficiently induce a coherent lattice motion, which can dynamically modify the optical properties of the transition metal oxide nanocrystals. The insight obtained here will also be a useful guide to the investigation of the possible dynamic modification of the magnetic properties in transition metal oxide nanocrystals via coherent lattice motions.

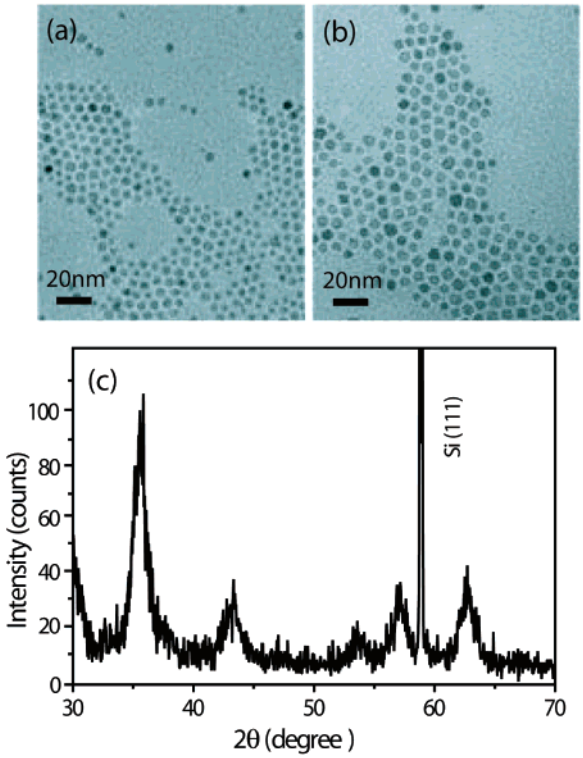

Figure 1. (a,b) Transmission electron micrographs of 4.8 and 8.3 nm γ-Fe_2O_3 nanocrystals. (c) X-ray diffraction pattern of γ-Fe_2O_3 nanocrystals. A sharp peak labeled as Si(111) is from the silicon substrate.

2. Experiments

Sample Preparation and Characterization. Two different sizes of spherical γ-Fe_2O_3 nanocrystals (4.8 and 8.3 nm in diameter, ~10% size dispersity) were synthesized by employing variations of the published procedures.[21,22] Briefly, Fe_3O_4 nanocrystals were initially synthesized by reducing Fe(acetylacetonate)$_3$ with a mixture of oleic acid, oleylamine, and 1,2-dodecandiol at 260 °C in octyl ether. Fe_3O_4 nanocrystals were cleaned and further oxidized to γ-Fe_2O_3 by heating in phenyl ether in the presence of oxygen. The resulting sample was characterized by using transmission electron microscopy (TEM), X-ray diffraction (XRD), and Raman scattering. Figure 1 shows TEM images and the XRD pattern of γ-Fe_2O_3 nanocrystals.

The absorption cross section of the nanocrystals was obtained by measuring the concentration of Fe^{3+} ion in the γ-Fe_2O_3 nanocrystal samples of known size and optical density. Inductive coupled plasma atomic emission spectroscopy was used to measure the Fe^{3+} concentration of the nanocrystal samples dissolved in hydrochloric acid. The size of the nanocrystals was obtained from the analysis of TEM images. The measured absorption cross sections for γ-Fe_2O_3 nanocrystals of two different sizes are shown in Figure 2a.

Pump−Probe Transient Absorption Measurement. Pump−probe transient absorption measurement was made on an amplified Ti:sapphire laser, which produced pulses of 60 fs centered at 780 nm at 3 kHz repetition rate. For the pump beam, either 780 nm fundamental or 390 nm doubled beam in β barium borate (BBO) were used. For the probe beam, a white light continuum generated by focusing 780 nm beam on a 2 mm thick

(14) Goldstein, A. N.; Echer, C. M.; Alivisatos, A. P. *Science* **1992**, *256*, 1425−1427.
(15) Son, D. H.; Hughes, S. M.; Yin, Y. D.; Alivisatos, A. P. *Science* **2004**, *306*, 1009−1012.
(16) Cerullo, G.; De Silvestri, S.; Banin, U. *Phys. Rev. B* **1999**, *60*, 1928−1932.
(17) Hartland, G. V. *Annu. Rev. Phys. Chem.* **2006**, *57*, 403−430.
(18) Son, D. H.; Wittenberg, J. S.; Banin, U.; Alivisatos, A. P. *J. Phys. Chem. B* **2006**, *110*, 19884−19890.
(19) Cherepy, N. J.; Liston, D. B.; Lovejoy, J. A.; Deng, H.; Zhang, J. Z. *J. Phys. Chem. B* **1998**, *102*, 770−776.
(20) Fu, L.; Wu, Z.; Ai, X.; Zhang, J.; Nie, Y.; Xie, S.; Yang, G.; Zou, B. *J. Chem. Phys.* **2004**, *120*, 3406−3413.
(21) Sun, S.; Zeng, H. *J. Am. Chem. Soc.* **2002**, *124*, 8204−8205.
(22) Woo, K.; Hong, J.; Choi, S.; Lee, H.-W.; Ahn, J.-P.; Kim, C. S.; Lee, S. W. *Chem. Mater.* **2004**, *16*, 2814−2818.

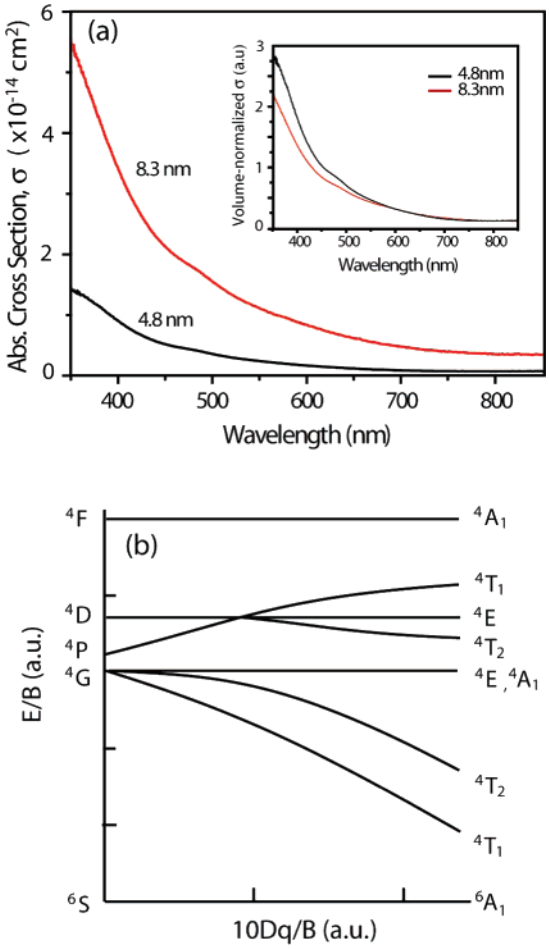

Figure 2. (a) Absorption cross section of 4.8 and 8.3 nm γ-Fe_2O_3 nanocrystals. Inset: Absorption cross section normalized to the volume of the nanocrystals. (b) Tanabe−Sugano diagram for Fe^{3+} in γ-Fe_2O_3.

sapphire crystal was used. The probe beam passed through a prism dispersion compensator, which was also used to preselect the wavelength of the probe light before the sample. Preselection of the probe wavelength greatly diminished the artifact near zero time delay arising from the cross-phase modulation under intense excitation. Typical pump−probe cross correlation and step size were 70 and 10 fs, respectively. Pump and probe beam diameters were 150 and 30 μm, respectively. The optical density at the pump wavelength was kept around 0.1 to minimize the variation of the pump intensity within the sample. The average pump fluence under the probe pulse area was varied between 8 and 80 mJ/cm^2 for studying pump fluence dependence, while most of the data reported here were obtained at the fluence of 80 mJ/cm^2.

γ-Fe_2O_3 nanocrystal samples were dispersed in cyclohexane and continuously circulated through a jet nozzle to produce a free streaming jet to ensure excitation of the fresh sample area for each pump pulse. The thickness of the sample jet was 400 μm. In metallic nanocrystals, intense excitations could induce thermal lensing or the formation of bubbles due to the very rapid electronic relaxation that heated the lattice and the surrounding solvent molecules.[23,24] However, combined with much slower electronic relaxation (∼100 ps) compared to the metal nanocrystals (several ps), the flowing jet was effective in preventing the problems arising from the rapid local solvent heating. X-ray diffraction data of the sample taken before and after a long period of measurements (typically 10 h) showed no indication of phase transition into α-Fe_2O_3 by continued exposure to the pump pulse.

3. Results and Discussion

Dynamic Features in Transient Absorption Data. Parts a and b of Figure 2 show the absorption cross sections of γ-Fe_2O_3 nanocrystals and Tanabe−Sugano diagram for the ligand field states of high-spin Fe^{3+} in the octahedral and tetrahedral coordination. A weak absorption at the pump wavelength (780 nm) is attributed to the forbidden transition from the ground ($^6A_1$) to the excited ($^4T_1$) ligand field state of Fe^{3+} ions. In the visible probe wavelength region, other forbidden ligand field transitions contribute to the absorption, including single and pair excitation of the ligand field transitions.[25] The stronger and allowed ligand-to-metal charge-transfer transition occurs at higher energies above 4 eV. The finite absorption intensities of all the ligand field transitions derive from the partial relaxation of the selection rules from the combination of spin orbit coupling, magnetic coupling of neighboring Fe^{3+} ions, and orbital mixing between Fe^{3+} and O^{2-} ions. In γ-Fe_2O_3, Fe^{3+} ions are located at both the octahedral and tetrahedral coordination sites, with approximately 3:2 site occupation ratio in bulk.[26] $^6A_1 \rightarrow {}^4T_1$ transition at the pump wavelength is spin- and Laporte-forbidden for Fe^{3+} at the octahedral site and only spin-forbidden for Fe^{3+} at the tetrahedral site. On the basis of this selection rule, Fe^{3+} at the tetrahedral site should have a stronger absorption at the pump wavelength, resulting in preferential excitation of Fe^{3+} at the tetrahedral coordination site. The selection rule may become more relaxed in small nanocrystals due to the deviation from the octahedral and tetrahedral ligand field symmetry for the surface Fe^{3+} ions. While this may have a non-negligible effect on the absorption intensities of the ligand field transitions, systematic studies on the effect of the surface atoms or spatial confinement of the electrons in nanocrystalline iron oxides are currently lacking.

Parts a and b of Figure 3 show the transient absorption data of spherical γ-Fe_2O_3 nanocrystals of the two different diameters (4.8 and 8.3 nm), pumped at 780 nm and probed at various visible wavelengths. In Figure 3, both sets of the data exhibit dynamics occurring on multiple time scales. In addition, intense oscillatory features from coherent phonons are superimposed on the decaying induced absorption at all probe wavelengths. The transient absorption data were well fit to a sum of exponential functions and an exponentially decaying cosine function. From this fit, the oscillatory and nonoscillatory features of the transient absorption data were separated to reveal the underlying dynamics more clearly as shown in Figure 4. Longer time scale dynamics at 550 nm probe wavelength is also shown in Figure 5. The main features in the dynamics are: (i) an immediate rise and decay of the pump-induced absorption in 100 fs, (ii) a build-up of the induced absorption in 1 ps at shorter probe wavelengths (e.g., 515, 550 nm), (iii) a decay of the

(23) Hu, M.; Petrova, H.; Hartland, G. V. *Chem. Phys. Lett.* **2004**, *391*, 220−225.
(24) Maillard, M.; Pileni, M.-P.; Link, S.; El-Sayed, M. A. *J. Phys. Chem. B* **2004**, *108*, 5230−5234.
(25) Sherman, D. M. *Phys. Chem. Miner.* **1985**, *12*, 161−175.
(26) Schwertmann, U.; Cornell, R. M. *The Iron Oxides*, 2nd ed.; Wiley-VCH: Weinheim, 2003.

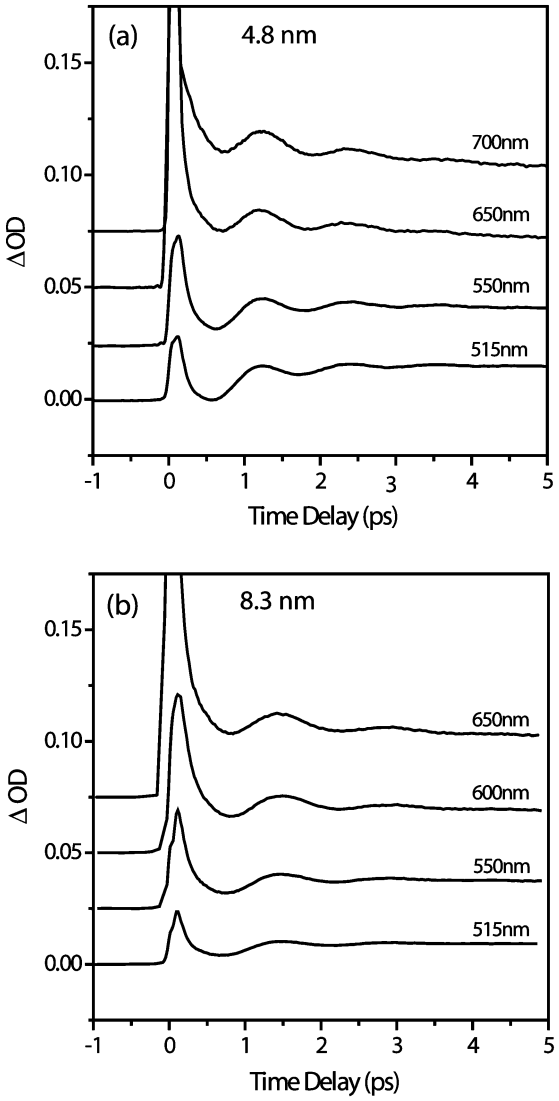

Figure 3. Transient absorption data of (a) 4.8 nm and (b) 8.3 nm γ-Fe_2O_3 nanocrystals pumped at 780 nm and probed at various wavelengths indicated above each set of data.

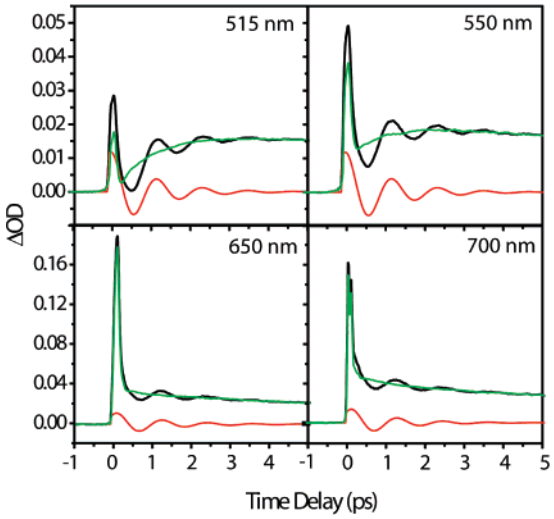

Figure 4. Transient absorption data of 4.8 nm γ-Fe_2O_3 nanocrystals. Oscillatory and nonoscillatory parts are separated to reveal the dynamics more clearly. Note different *y*-scales for upper and lower panels. Probe wavelength is indicated in each panel. Original transient absorption data (black), $A\cdot\cos(2\pi t/\tau + \phi)$ function to fit the oscillatory part (red), oscillation-subtracted data (green).

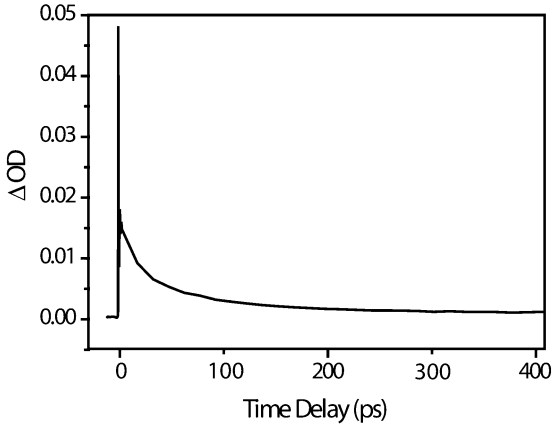

Figure 5. Long-time window transient absorption data of 4.8 nm γ-Fe_2O_3 nanocrystals obtained with 780 pump and 550 nm probe.

induced absorption on 17 and 100 ps time scale with 15 and 85% amplitude, respectively, and (vi) prominent oscillations with a size-dependent period.

From the absorption cross section of γ-Fe_2O_3 nanocrystals at the pump wavelength measured in a separate experiment ($\sigma = 7.1 \times 10^{-16}$ cm^2 for 4.8 nm nanocrystal), it was estimated that about 10% of the Fe^{3+} ions in each nanocrystal were excited at the pump fluence of 80 mJ/cm^2. With this estimation and the oscillation-subtracted transient absorption traces, absorption spectra of the excited state at several time delays were constructed by using the following equation,

$$\Delta OD(t,\lambda) = x(t)\cdot[OD_e(t,\lambda) - OD_g(\lambda)] \qquad (1)$$

where $\Delta OD(t,\lambda)$ is the oscillation-subtracted transient absorption signal at time t, $x(t)$ is the average fraction of the excited Fe^{3+} ions in each nanocrystal, $OD_e(t,\lambda)$ and $OD_g(\lambda)$ are the excited- and ground-state absorption of the nanocrystal, respectively. In using eq 1, we assumed that the absorption cross section of each nanocrystal for the ligand field transitions can be roughly represented as a sum of contributions from all local absorbing Fe^{3+} ions. This may be more readily justified for the transitions below the band gap (2.2 eV)[26] that are considered predominantly localized on each Fe^{3+} ion. The above assumption is consistent with our measurement of the absorption cross sections of γ-Fe_2O_3 nanocrystals of different sizes. The absorption cross section normalized to the volume of the nanocrystal, shown in the inset of Figure 2a, is insensitive to the size of the nanocrystal especially below the band gap ($\lambda < 560$ nm).

In Figure 6, the calculated $OD_e(t,\lambda)$ are plotted together with $OD_g(\lambda)$. The excited-state absorption, right after the excitation, is significantly more intense than the ground-state absorption, particularly in longer probe wavelength region. After the initial fast decay, the excited-state absorption decreases and shows a flatter spectrum. The excited state has more intense absorption than the ground state because all the ligand field states except the ground state have the sample spin multiplicity, which lifts the restriction imposed by the spin selection rule.

Ultrafast Energy Transfer and Relaxation Dynamics of Ligand Field State. In this section, we discuss the dynamic features of the oscillation-subtracted transient absorption data. In Figure 4, the immediate rise and fast (100 fs) decay of the induced absorption are observed in the entire range of the probe

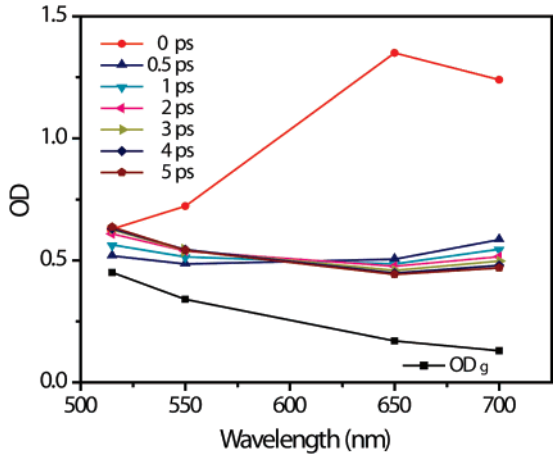

Figure 6. Ground-state absorption (OD_g) and excited-state absorption (OD_e) spectra constructed by using eq 1 at several different delay times.

wavelengths covered in this study, from 515 to 700 nm. This indicates that part of the initially excited-state relaxes immediately after the excitation. The fast-decaying component was also observed in the transient absorption data obtained with 390 nm (3.1 eV) excitation in earlier study by Cherepy el al.[19] In their study, <100 fs decay of the pump-induced absorption was attributed to the relaxation of hot electrons following the above-band gap (E_g = 2.2 eV) excitation. Initial <100 fs relaxation was followed by a slower decay on tens of picoseconds time scale, which was attributed to the relaxation from the conduction band edge to the valence band. However, the initial 100 fs decay observed in this study cannot be explained in the same way as with 390 nm excitation because the conduction band cannot be reached by the one-photon excitation. The transient absorption signal was linear or slightly sublinear to the pump fluence within the fluence range of this study (8−80 mJ/cm^2), showing no indication of the two-photon, above-band gap excitation. The possibility of the artifact from coherent pump−probe coupling was ruled out, although it can obscure the early time dynamics under certain circumstances. The initial 100 fs decay component was consistently observed for both parallel and perpendicular pump−probe polarizations. Even though the coherent artifact was observed for parallel pump−probe polarization with small pump−probe detuning (e.g., 780/700 pump−probe), it was distinguishable from the rest part of the data.

Several relaxation pathways can be considered to account for the initial fast relaxation dynamics of the excited state; immediate trapping of the excited state to nearby quenching sites such as the octahedral vacancies or the surface, relaxation within the vibronic manifold of the excited state, and the energy transfer to other lower energy Fe^{3+} ions. Trapping of the excited state to the defect site within the lattice or on the surface was suggested as one of the relaxation pathways in a number of semiconductor and metal oxide nanocrystals, typically from the conduction band, occurring on a picosecond time scale or longer.[27−29] For the ligand field transition at 780 nm, which is mainly localized to Fe^{3+} ions and already low in energy, it is unlikely that the significant portion of the initial excitation will be trapped in 100 fs. However, trapping to the defect sites may become increasingly important at higher excitation intensities, where multiphoton excitation to the higher energy states becomes possible.

Relaxation within the vibronic manifold of the excited state is also not likely to occur in 100 fs because that process also takes a picosecond or longer in typical solids.[30] Moreover, there is a component of the dynamics relaxing on ∼1 ps time scale following 100 fs initial decay, which can be more readily associated with the vibrational relaxation.

A further insight into the fast initial relaxation can be obtained from the following consideration. As discussed in the previous section, the 780 nm pump may preferentially excite $^4T_1$ state of the Fe^{3+} ion at the tetrahedral coordination site. According to the earlier studies on the ligand field transition energies of oxo-coordinated Fe^{3+} ions, the energy level of the $^4T_1$ state at the octahedrally coordinated Fe^{3+} ion lies below that of the tetrahedral coordination site.[25,31] This can allow the energy transfer from the tetrahedral to octahedral Fe^{3+} ions. On the other hand, relatively small absorption intensities[32] near the pump wavelength argue against the effective energy transfer via dipolar interaction. However, the short distance between the octahedral and tetrahedral sites (the nearest-neighbor distance = 3.45 Å) can allow the effective energy transfer via exchange interaction between the two Fe^{3+} centers. Such exchange interaction-mediated energy transfer was previously observed in cobalt complexes between the ligand field states centered on different metal centers and in bichromophoric molecules.[33,34] On the basis of the above discussion, the fast initial decay of the induced absorption in 100 fs has been assigned to the energy transfer from the tetrahedral $^4T_1$ to octahedral $^4T_1$ states. This assignment is also consistent with a sharp decrease instead of the build-up of the excited-state absorption throughout the visible region. While the transitions from $^4T_1$(tetrahedral) to the upper states are both spin- and orbital-allowed, transitions from $^4T_1$-(octahedral) are only spin-allowed. This should result in a decrease in the excited-state absorption intensity after the energy transfer from the tetrahedral to octahedral Fe^{3+} center as observed in this study.

A closer look at the oscillation-subtracted transient absorption data (Figure 4) reveals that the induced absorption rises on a 1 ps time scale at 515 and 550 nm probe wavelengths, while it continues to decrease at longer wavelengths. Subsequently, the broad induced absorption decays multiexponentially on 17 and 100 ps time scales with 15% and 85% amplitude, respectively. The apparent blue-shift of the excited-state absorption on a 1 ps time scale can be attributed to the relaxation within the vibronic manifold after the energy transfer. A similar assignment has been made earlier by Juban et al.[35] in a transition metal complex with an octahedrally coordinated Cr^{3+} center. In their study, the dynamics occurring on a 1.1 ps time scale was attributed to the relaxation in the vibronic manifold of the ligand field state following the ultrafast intersystem crossing from a

(27) Klimov, V.; Bolivar, P. H.; Kurz, H. *Phys. Rev. B* **1996**, *53*, 1463−1467.
(28) Colombo, D. P.; Roussel, K. A.; Saeh, J.; Skinner, D. E.; Cavaleri, J. J.; Bowman, R. M. *Chem. Phys. Lett.* **1995**, *232*, 207−214.
(29) Zhang, J. Z. *J. Phys. Chem. B* **2000**, *104*, 7239−7253.
(30) Hill, J. R.; Chronister, E. L.; Chang, T. C.; Kim, H.; Postlewaite, J. C.; Dlott, D. D. *J. Chem. Phys.* **1988**, *88*, 949−967.
(31) Sherman, D. M.; Waite, T. D. *Am. Mineral.* **1985**, *70*, 1262−1269.
(32) Molar extinction coefficient per Fe^{3+} ion was calculated to be ∼80 M^{-1} cm^{-1} for the iron oxide nanocrystals used in this study.
(33) Kane-Maguire, N. A. P.; Allen, M. M.; Vaught, J. M.; Hallock, J. S.; Heatherington, A. L. *Inorg. Chem.* **1983**, *22*, 3851−3855.
(34) Mondal, J. A.; Ramakrishna, G.; Singh, A. K.; Ghosh, H. N.; Mariappan, M.; Maiya, B. G.; Mukherjee, T.; Palit, D. K. *J. Phys. Chem. A* **2004**, *108*, 7843−7852.
(35) Juban, E. A.; McCusker, J. K. *J. Am. Chem. Soc.* **2005**, *127*, 6857−6865.

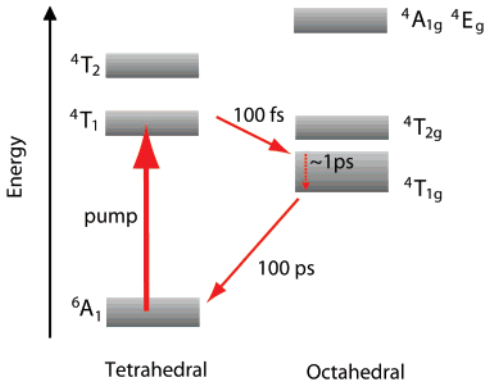

Figure 7. Simplified energy level diagram and the assignment of the dynamics.

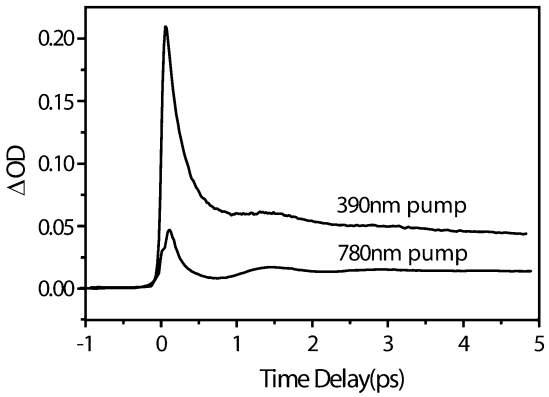

Figure 8. Comparison of the transient absorption data obtained with 390 and 780 nm pump and 550 nm probe for 8.3 nm γ-Fe_2O_3 nanocrystals.

charge transfer to a ligand field state. With the foregoing assignments of the dynamics, the slow relaxation on 100 ps time scale, which carries 85% of the decay amplitude, can be assigned to the relaxation of $^4T_{1g}$ state to the ground state. The nature of 17 ps decay dynamics is not clear at the moment, although it may be assigned to earlier phase of electronic relaxation. The assignments of the dynamics observed in the transient absorption data are summarized in Figure 7.

Creation of Coherent Phonon from Ligand Field Excitation. The oscillatory features in the transient absorption data indicate creation of coherent phonons by the optical excitation. Coherent phonons are usually excited by either displacive or impulsive mechanism depending on the electronic structure of the sample and the properties of the excitation pulse.[36,37] For γ-Fe_2O_3 nanocrystals excited at 780 nm, the coherent phonon is likely to be created through the displacement of the equilibrium lattice geometry upon $^6A_1 \rightarrow {}^4T_1$ excitation rather than impulsive stimulated Raman scattering by considering the cosine phase of the oscillation. One might expect that the excitation of a coherent phonon through the below-band gap ligand field transition is rather inefficient because it is considered to be predominantly localized on the metal ions, unlike charge-transfer transitions. According to the theoretical calculations on a few transition metal complexes, the ligand field transitions have 5−10 time smaller vibronic coupling than the charge-transfer transitions between the metal and ligand.[38,39] Nevertheless, the weak vibronic coupling in the ligand field transition seems to be sufficient to excite a coherent phonon in the lattice of γ-Fe_2O_3 nanocrystals. The origin of the displacement of the equilibrium geometry from $^6A_1 \rightarrow {}^4T_1$ transition is the change of the electronic configuration in d-orbitals that shifts one electron from an antibonding to a nonbonding molecular orbital.[25] This will result in the decrease in the metal−ligand equilibrium distance upon excitation to $^4T_1$ state. Although the contraction of the lattice in the excited state of γ-Fe_2O_3 has not been experimentally observed yet, recently developed tools such as time-resolved X-ray absorption or diffraction will be particularly suitable for making such a measurement.[11,40]

The oscillation in the transient absorption was also observed when 390 nm excitation pulses were used, which essentially excites the higher-lying ligand field states. The oscillation periods and the phases were the same in both 390 and 780 nm excitation. (Figure 8). In previous studies on the ultrafast dynamics of the photoexcited iron oxide nanocrystals using 390 nm excitation, the oscillations due to coherent phonons were not observed. This is probably due to the broad size distribution of the nanocrystals and insufficient signal/noise ratio.

The period (τ) of the oscillation was dependent on the radius (r) of the nanocrystals, where $\tau = 1.1$ and 1.5 ps for $r = 2.4$ and 4.2 nm, respectively. The phonon mode responsible for the oscillation of the absorption intensity is most likely the lowest-order radially symmetric mode of confined acoustic phonon.[16] The size dependence of coherent acoustic phonon in nanocrystals has been usually explained by Lamb's theory of the confined acoustic mode in the spherical elastic particles.[41] For the lowest-order radial breathing mode, the period (τ) of acoustic phonon can be calculated from eq 2, which predicts a linear relationship between the radius (r) of the particle and the period (τ) of phonon.

$$\tau = \frac{2\pi r}{\eta c_L}, \qquad \eta \cot(\eta) = 1 - \left(\frac{\eta c_L}{2 c_T}\right)^2 \tag{2}$$

c_L and c_T are the longitudinal and transverse speed of sound, respectively, which are related to the Young's moduli (C_{11} and C_{44}) and the density (ρ) through $c_L = \sqrt{C_{11}/\rho}$, $c_T = \sqrt{C_{44}/\rho}$. Because of the lack of information on the Young's moduli of γ-Fe_2O_3, we could not compare the measured periods with the predictions from Lamb's theory. However, the period of the oscillation was within the typical range that would be expected for the materials of similar structure.[42,43] While Lamb's theory predicts a linear relationship between the vibrational period and the size of the particle, the experimental result deviates from this prediction. This is probably due to the variation of the Young's moduli of γ-Fe_2O_3 with the size in the nanometer range, where the fraction of the surface atoms is a strong

(36) Zeiger, H. J.; Vidal, J.; Cheng, T. K.; Ippen, E. P.; Dresselhaus, G.; Dresselhaus, M. S. *Phys. Rev. B* **1992**, *45*, 768−778.
(37) Pollard, W. T.; Dexheimer, S. L.; Wang, Q.; Peteanu, L. A.; Shank, C. V.; Mathies, R. A. *J. Phys. Chem.* **1992**, *96*, 6147−6158.
(38) Aramburu, J. A.; Moreno, M.; Doclo, K.; Daul, C.; Barriuso, M. T. *J. Chem. Phys.* **1999**, *110*, 1497−1507.
(39) Harris, D.; Loew, G. H.; Komornicki, A. *J. Phys. Chem. A* **1997**, *101*, 3959−3965.
(40) Gawelda, W.; Pham, V.-T.; Benfatto, M.; Zaushitsyn, Y.; Kaiser, M.; Grolimund, D.; Johnson, S. L.; Abela, R.; Hauser, A.; Bressler, C.; Chergui, M. *Phys. Rev. Lett.* **2007**, *98*, 057401−057404.
(41) Lamb, H. *Proc. Math. Soc. London* **1882**, *13*, 187.
(42) The period calculated for 4.8 nm γ-Fe_2O_3 nanocrystal using Young's moduli of Fe_3O_4 obtained from ref 43 was 1.3 ps. Both Fe_3O_4 and γ-Fe_2O_3 have the same inverse spinel structure.
(43) *Mineral Physics and Crystallography: A Handbook of Physical Constants*; American Geophysical Union: Washington DC, 1995.

function of the size. Indirect evidence for the size-dependent Young's moduli can be obtained from the size-dependent bulk modulus.[44] The bulk modulus of γ-Fe_2O_3 nanocrystals measured under the hydrostatic pressure increased with the radius of the nanocrystal, which suggests a similar size dependence of the Young's moduli. According to this assumption, the Young's moduli of 8.3 nm nanocrystal are about 35% larger than 4.8 nm nanocrystal. This can partly explain the sublinear relationship between the radius and the oscillation period observed in this study.

Strong Modulation of Oscillator Strength by Coherent Phonon. The oscillation in the transient absorption, whose amplitudes is as large as ΔOD, seems unusually intense for the transitions exhibiting rather broad and featureless absorption spectra in both the ground and excited states. This is particularly intriguing, considering the relatively small vibronic coupling of the ligand field transitions compared to the charge-transfer transitions. In fact, coherent excitation of the vibrational modes in transition metal complexes via the ligand field excitation was observed only rarely, e.g., in blue copper proteins, whose ligand field transition borrows an intensity significantly from the charge-transfer transtion.[45]

For more quantitative analysis of the oscillation amplitude, we calculated the relative amplitude of the oscillation with respect to the total absorption intensity (OD) at a given time delay. $OD(t,\lambda)$ was calculated simply from the following equation

$$OD(t,\lambda) = \Delta OD(t,\lambda) + OD_g(\lambda) \qquad (3)$$

where ΔOD and OD_g are defined in the same way as in eq 1. As discussed in the previous section, we estimated that about 10% of the total Fe^{3+} ions in each nanocrystal were excited initially based on the measured absorption cross section and the pump fluence. Under this condition, the modulation of the absorption was 1−6% of the total absorption (OD) depending on the probe wavelength.[46] The modulation depth also increased linearly to the pump fluence within the fluence range of 8−80 mJ/cm^2, as shown in Figure 9. This indicates that excitation of each Fe^{3+} ion modulates 10−60% of its contribution to the total absorption intensity of the nanocrystal within the pump fluence range of our study.

Another notable feature is the wavelength dependence of the modulation depth. Typically, coherent phonons or vibrational wavepackets in crystalline solids and molecules shift only the band gap or the peak of the absorption spectrum periodically without changing the oscillator strength. In this case, the relative amplitude and phase of the oscillations at different probe wavelengths reflect the slope of the absorption spectrum.[37] For γ-Fe_2O_3 nanocrystals, the observed modulation depth is too large to be explained simply by the periodic shift of the relatively flat ground and excited absorption spectra, particularly at the longer wavelength region. Furthermore, the oscillation amplitude increases with the probe wavelength, while the slope of the absorption spectra decreases with the wavelength or show a flat

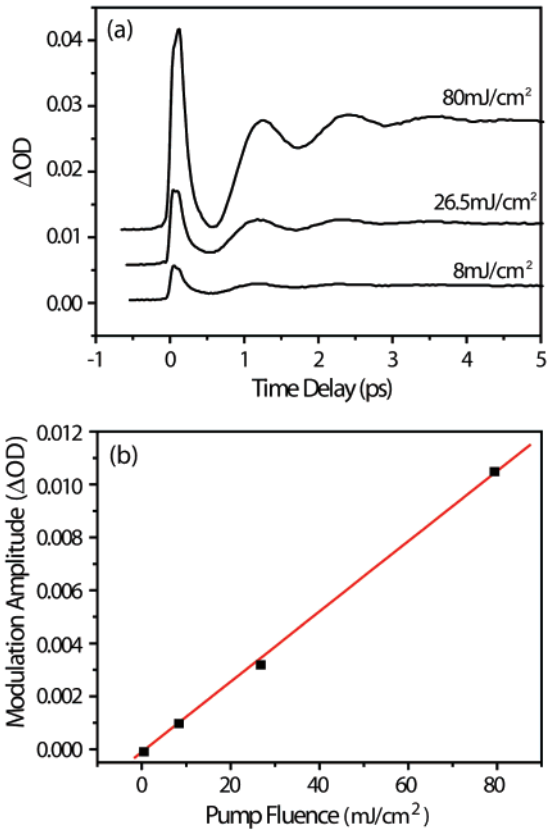

Figure 9. (a) Pump fluence dependence of the transient absorption data with 780 nm pump and 550 nm probe for 4.8 nm γ-Fe_2O_3 nanocrystals. (b) Pump fluence dependence of the oscillation amplitude.

shape, as shown in Figure 6. This suggests that the oscillations in the transient absorption are primarily due to the modulation of the oscillator strength rather than the oscillating Frank−Condon overlap.

Strong modulation of the oscillator strength in γ-Fe_2O_3 nanocrystals by coherent acoustic phonon can be qualitatively understood from the following consideration. Metal−ligand orbital overlap and the exchange interaction between the metal ions are among the important factors that determine the intensity of the forbidden ligand field transitions.[47] Because the magnitudes of those factors are dependent on the metal−ligand distance, metal−metal distance, and metal−ligand−metal angle, coherent phonon can modify the oscillator strength of the ligand field transitions.[48] Time-dependent symmetry breaking of the ligand field may also play a role. A similar modulation of the oscillator strength by vibrational wavepacket was previously observed in a few molecular systems, where the creation of the wave packet was coupled to a charge transfer or an exciton transition.[49,50] This interpretation is also consistent with the pressure dependence of the ligand field transition energy and intensity observed for a number of transition metal complexes in a study done by Drickamer et al.[51] In their study, the oscillator strength of the ligand field transition increased with the pressure, which changes the metal−ligand distance and distorts the lattice

(44) Clark, S. M.; Prilliman, S. G.; Erdonmez, C. K.; Alivisatos, A. P. *Nanotechnology* **2005**, *16*, 2813−2818.
(45) Book, L. D.; Arnett, D. C.; Hu, H.; Scherer, N. F. *J. Phys. Chem. A* **1998**, *102*, 4350−4359.
(46) The modulation depth was calculated using the amplitude (A) of the exponentially decaying cosine function $A\cos(2\pi t/\tau + \phi)$, which describes the oscillatory part of the transient absorption data.
(47) Lehmann, G. *Chem. Phys. Lett.* **1979**, *65*, 184−186.
(48) Weihe, H.; Gudel, H. U. *J. Am. Chem. Soc.* **1997**, *119*, 6539−6543.
(49) Kano, H.; Saito, T.; Kobayashi, T. *J. Phys. Chem. A* **2002**, *106*, 3445−3453.
(50) Son, D. H.; Kambhampati, P.; Kee, T. W.; Barbara, P. F. *J. Phys. Chem. A* **2002**, *106*, 4591−4597.
(51) Parsons, R. W.; Drickamer, H. G. *J. Chem. Phys.* **1958**, *29*, 930−937.

structure. Although the data from such measurements are not available for γ-Fe_2O_3 nanocrystals, it is reasonable to expect a similar behavior in γ-Fe_2O_3 nanocrystals.

Finally, it is noteworthy to compare the influence of coherent phonons on transition metal oxide nanocrystals with those on metal and semiconductor nanocrystals. For many metal and semiconductor nanocrystals, relatively simple changes in the energy band structure can usually explain the effect of coherent phonons on the optical properties via periodic shift of the plasmon resonance or band gap.[13,17] On the other hand, the effect can be more pronounced and complex in transition metal oxide nanocrystals. Multiple factors, such as the metal−ligand orbital overlap, magnetic interaction between the metal ions, and dissymmetry of the ligand field, can affect the properties of forbidden ligand field transitions with a varying sensitivity. Additionally, coherent phonons may also influence the magnetic properties of the transition metal oxide nanocrystals. Because the magnetic moment has it origin also on the unpaired d-electrons, periodic modulation of the metal−ligand distance may redistribute the spin density, thereby changing the magnetic moment on the metal ions.[52,53]

4. Concluding Remarks

Relaxation dynamics of an optically excited ligand field state and the effect of the coherent phonon on the intensities of ligand field transitions in γ-Fe_2O_3 nanocrystals were investigated. We were interested in studying the dynamics of the optical transitions in γ-Fe_2O_3 nanocrystals, particularly following the excitation of the ligand field state, due to the capability of directly modifying the electronic and spin states of d-electrons. According to the spin- and orbital-selection rules, near-infrared pump pulse preferentially excite the Fe^{3+} ions in the tetrahedral coordination sites. The excited ligand field state exhibited an ultrafast (100 fs) energy transfer to the neighboring octahedral Fe^{3+} ions and subsequently went through the vibrational and electronic relaxation. Furthermore, the ligand field excitation created a coherent acoustic phonon, resulting in strong oscillations in the transient absorption data. While the ligand field excitation is considered to be predominantly localized to Fe^{3+} ions and weakly coupled to the lattice modes, modulation of the absorption by an coherent acoustic phonon was very intense. The strong oscillation of the absorption has been explained in terms of the modulated oscillator strength of the ligand field transitions. The present observation demonstrates that the ligand field excitation can create coherent phonons in the transition metal oxide nanocrystals, which can dynamically modify their material properties.

Acknowledgment. This work was supported by a Texas A&M University start-up grant and the Robert A. Welch Foundation (A-1639). We thank the Microscopy & Imaging Center of Texas A&M University for electron microscopy and Professor Timothy Hughbanks for helpful discussions.

JA072578F

(52) Pillet, S.; Souhassou, M.; Lecomte, C. *Acta Crystallogr., Sect. A: Cryst. Struct. Commun.* **2004**, *60* 455−464.
(53) Vanloef, J. J. *Physica* **1966**, *32*, 2102−2114.